Practical Paper

The practical application of computational fluid dynamics to dissolved air flotation, water treatment plant operation, design and development

Tony Amato and Jim Wicks

ABSTRACT

Computational fluid dynamics (CFD) can be applied to the advancement of dissolved air flotation (DAF) plant design. The use of CFD in design and predictive analysis, in particular here with reference to the upgrading of an existing DAF plant from 30 to 60 Ml/d and associated diagnostics, while still developing, helped by the emergence of ever more powerful computational systems, can be regarded as an established tool providing beneficial and useful data, although on occasions care may be required in the interpretation of results. The initial CFD studies were undertaken using the existing and upgraded works flows and structures at both 'low' and 'high' temperatures, i.e. 2 and 20°C, while the modelling results are reported using graphical representations of 'contours of flow velocity' and 'velocity vectors'. In addition the degree of short circuiting based on T_{10} together with other retention parameters T_{50} and T_{50}/m are reported. Further modifications were also considered: how changes to the incline baffle and tank depth can impact on the predicted distribution, vorticity and in practice on the actual subnatant water quality measured in terms of turbidity. Finally applying CFD to DAF plant design is shown to be a beneficial tool for the designer.

Key words | computational fluid dynamics, dissolved air flotation, water treatment

Tony Amato
Enpure Ltd, Enpure House,
Woodgate Business Park,
Kettleswood Drive,
Birmingham B323DB,
UK
E-mail: *tamato@enpure.co.uk*

Jim Wicks
The Fluid Group, Magdalen Centre,
The Oxford Science Park,
Oxford OX44GA,
UK
E-mail: *jim.wicks@thefluidgroup.com*

INTRODUCTION

The traditional approach to water treatment plant design is to consider a number of parameters such as but not limited to the capacity, processes to be applied, the general arrangement to assess land area requirements and water quality. All of these requirements, even to some extent the final water quality, are further constrained by the inevitable budgetary limitations placed on any project.

Where the proposals involve the building of a new plant the latest design know-how and approach can generally be applied without any major restrictions subject to the above limitations. However where an existing plant is to be upgraded and incorporated into any final design then one or more aspects of the latest available technological features may need to be adjusted to maximise the benefits within the constraints of the existing structures and layout.

It is this case which will be covered by this paper, which focuses on the improvements to the DAF clarification stage of Rosebery Water Treatment Works (WTW), an existing plant designed to produce 30 Ml/d and built in the early 1980s, located in the East Lothian region of Scotland near Edinburgh. While details are provided in Tables 1 and 2 on the two raw water reservoir sources that could be fed to the works together with the subnatant water quality specified and guaranteed for the upgraded plant, respectively, the specific water chemistry, flocculation and other treatment requirements throughout the water

doi: 10.2166/aqua.2009.003

Table 1 | Gladhouse and Megget Reservoir water quality supplied to Rosebery (1999–2003)

	Gladhouse					Megget				
	Ave.	Max	Min	St. Dev.	95%ile	Ave.	Max	Min	St. Dev.	95%ile
pH	7.54	8.10	7.00	0.25	7.90	7.30	8.00	6.30	0.38	7.90
Turbidity [NTU]	3.59	29.10	0.70	4.89	8.83	1.18	10.90	0.40	1.72	2.05
True colour [$mg\,l^{-1}$ Pt/Co]	33.32	56.00	19.00	9.13	47.00	19.61	46.00	13.00	5.33	23.00
Alkalinity [$mg\,l^{-1}$ as $CaCO_3$]	24.42	32.79	17.21	3.18	29.18	9.44	23.77	6.56	2.68	9.84
Conductivity [$\mu S\,cm^{-1}$]	81.44	102.00	73.00	5.71	87.45	42.08	75.00	35.00	6.01	45.00

temperature range 2–20°C reported, will not form part of this paper. The detail is provided here to simply highlight the nature of the water, which could be delivered in any combination, to be treated.

It should also be noted that, throughout this paper, the DAF loading rates quoted will be based on the flow per cell divided by its area, including both the contact and clarification zones as highlighted in Figure 1 but excluding any recycle flow.

PROJECT STRATEGY

The Rosebery plant was upgraded in accordance with the issued specification which required the works capacity to be increased from 30 to 60 Ml/d using where possible existing structures and processes. The latter was suitably upgraded to incorporate changes in technology since the plant was originally constructed. The original plant comprised an inlet mixing chamber which discharged into a common distribution channel, feeding three separate streams. Each stream comprised two stages of flocculation, providing a total of 20 minutes' retention at maximum design flow, followed by a close coupled DAF cell rated at a net loading of $10\,m\,h^{-1}$. The clarified or subnatant water then discharged via a fixed outlet weir arrangement into a common collection channel which fed four mono-media rapid gravity filters (RGF).

It had been envisaged in the project scoping document that the increased capacity would be achieved by simply doubling up on the main process streams, i.e. six and eight DAF and RGFs respectively, and a similar increase to all other ancillary equipment such as the DAF recycle system. However as part of the initial design review the possibilities of utilising the high rate DAF concepts reported by Edzwald *et al.* (1999) and Amato *et al.* (2001) were considered. As part of a feasibility study a full-scale site trial, over eight days was undertaken at a rate, limited by the maximum capacity of the recycle system, of ~150% design capacity, without any attempt to optimise the prevailing operating conditions. The results of this trial showed that at ~13°C subnatant turbidities were stable at ~1.6 NTU which compared favourably with pre-trial values of 1.4–2.5 NTU when only actually operating at 90% of design. In light of these results and improvements envisaged as part of any upgrade it was decided to incorporate the high rate concepts without further testing or modelling. The principle design parameters to be used were those of reduced flocculation times and increased DAF loadings where the total flocculation times could be reduced from 20 to 10 minutes and the net DAF loading could be increased from 10 to $20\,m\,h^{-1}$. There was no change to the amount of recycle required which remained equivalent to 6–10% of the incoming flow. As a result of applying the high rate concepts the need to build three additional DAF streams was removed and therefore a significant saving in project costs was attained.

Table 2 | Upgrade plant specified subnatant guaranteed water quality

Parameter	Value	Parameter	Value
Turbidity [NTU] (95%ile)	≤1.5	Soluble aluminium [$\mu g\,Al\,l^{-1}$]	≤50
Turbidity [NTU] (100%ile)	≤2.0	True colour [$mg\,l^{-1}$ Pt/Co]	≤5

As part of any design there are a number of areas that need to be considered and in incorporating certain local velocities the requisite flow patterns are attained thereby ensuring both good design and performance: these are summarised in Figure 1.

The Rosebery plant was upgraded in line with the detail referred to above and as each stage was completed hydraulic and process tests were undertaken to confirm that the design basis worked. During the course of these

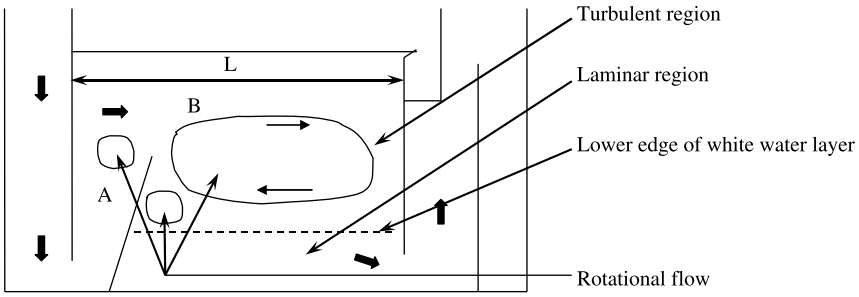

Figure 1 | Typical DAF design. 'A', the 'contact zone' where hydraulic retention times (HRT) are typically 60–240 seconds and rates are 20–110 m h^{-1}; 'B', generally referred to as the 'clarification zone' where the upper cross-flow velocities are generally <0.05 m s^{-1} including any circulation currents; loading rates are a function of influent and tank dimensions, i.e. length (L) and width.

tests one specific parameter was found to be higher than expected and this was the subnatant turbidity which only just achieved the 95%ile limit. In an attempt to improve operational flexibility a series of further investigations was undertaken to try to eliminate the possible sources contributing to the higher than expected turbidities. These investigations included the traditional optimisation of treatment chemistry via jar tests and process plant, such as the adjustment of flocculator speeds. While all of these gave some improvement, more was sought to mitigate the risk of exceeding the guarantee limits over an annual cycle.

As has already been stated there is always the likelihood that some limitation will be placed on any design when trying to incorporate the latest approach using pre-existing structures, which, while complying with theoretical requirements, do not appear to deliver what is expected. It was therefore considered appropriate at this time to use modelling techniques provided by the use of CFD, to look in particular at the baffling arrangement and flow patterns within the DAF cell with the basic dimensions detailed in Table 3.

PLANT MODELLING

The CFD modelling used was that based on a dynamic, second order, multiphase Eulerian-Eulerian renormalisation group k-epsilon (RNG $k-\varepsilon$) turbulent model (Marshall & Bakker 2002), simulating both water (temperature within the specified range of 2–20°C) and air.

Table 3 | DAF cell dimension summary

Parameter	Value	Parameter	Value
Cell length [m]	5.34	Incline baffle angle [°]	80
Width [m]	7.7	Water depth [m]	2.391
Incline baffle vertical height [m]	1.136	Overall depth [m]	3.0

Background

While the mathematical equations and their manipulation fall outside the scope of this paper, the following is intended to highlight some of the mechanisms involved in the computational process.

In general CFD models and calculations will utilise first principles described by the Navier-Stoke equations of mass, momentum and energy conservation. In turn the models for multiphase flows can be divided into a number of categories; however, for these studies the use of the Eulerian-Eulerian model was selected as this is the most commonly used and acceptable under the conditions investigated and is based on the assumption of inter-penetrating continua. In addition it has been shown to be applicable for both continuous-continuous and continuous-dispersed systems, with the latter allowing the dispersed phase to be in the form of bubbles and hence appropriate for studying DAF.

A further consideration in determining the type of model to use is the turbulence associated with any flow through the DAF cell, since in these regions there will be fluctuations in both velocity and other parameters. Therefore for the model to be representative these need to be incorporated. To achieve this there are two equations in general and popular use when determining the impact of transport (i.e. velocity) and hence stress in terms of Reynolds. These equations, which are predominantly empirically based, need to be solved for the kinetic energy of turbulence 'k' and the rate of dissipation of that turbulence 'ε'.

In time and in an effort to rationalise the empirical nature of this approach the RNG model was developed (Yakhot & Orszag 1986). This model allowed for the effect of flows around bends or zones of recirculation rotational flow, which can be present within a standard DAF cell.

Once the occurrence of rotational flow is recognised within the DAF cell, as highlighted in Figure 1, its impact on the ultimate product water quality should be considered. However, in an attempt to quantify this, the degree of rotation needs to be determined. It was concluded that this was best determined by a measure of the vorticity, where a value greater than zero indicates some degree of rotation. The more intense the degree of rotation the greater is the likely risk of disturbance of the bubble floc agglomerate and in turn an increased risk that the subnatant exiting the DAF cell will have a higher than desired turbidity.

Mathematically vorticity (ξ), a vector quantity, is defined as the curl or rot (∇) of the velocity vector (U) (i.e. $\xi = \nabla \times U$). The units of vorticity are the same as the shear rate, that of s^{-1}, where a negative or positive value within a volume merely indicates that rotational direction is different or opposite.

As part of the rationale used in this paper to assess the results, reference has been made to the 'volume weighted average' vorticity magnitude, as given by Equation (1), where ψ denotes the scalar variable of vorticity.

$$\frac{1}{V}\int \psi \, dV = \frac{1}{V}\sum_{i=1}^{n} \psi_i |V_i| \quad (s^{-1}) \tag{1}$$

Methodology

The first models, both 2D and 3D, were constructed in Fluent 6.2.16 and consisted of 335,000 hexahedral cells. Later, further models were built in 2D (double precision) using Fluent 6.3.26 to simulate increasing the tank depth.

While all the initial studies were carried out in 3D, owing to the onerous computational requirements of 3D and in part to simplify the iterations involved in assessing various scenarios, it was decided to use predominantly 2D results for comparative purposes.

Furthermore, noting the possible coupling effects of the flow through the latter stages of flocculation, which can impact on the uniformity of the flow into the DAF cell, with potentially higher localised velocities promoted by the actual flocculator configuration, these effects within the context of this paper have been ignored. It has been assumed that, while the lack of uniformity may alter the absolute values of any 3D results, the relative values across all models from this will remain unchanged, particularly as the total flow and flocculator conditions remain constant.

The recycle nozzles and main inlet flow were set as velocity inlets. The actual nozzle arrangement in terms of the modelling was dependent on whether 2D or 3D was being considered. In the first instance a simple nozzle set up was used, assuming an orifice in the horizontal plane. Second, in the case of the 3D models, the actual design and installed distribution headers and pipework were included. The top water surface boundary is defined as a frictionless wall. A gas sink (Ta *et al.* 2001) was applied at the surface to remove air from the domain at a rate equal to the flux across the water surface. Gravity is a downward force across the domain. The basic recycle fraction as a proportion of the inlet flow was 10% and bubble sizes of 70–100 μm at 10°C and 20°C were modelled.

A number of scenarios based on two phase conditions were investigated and these focused on: 1) a review of the impact of the length/height of the incline baffle, which effectively creates the exit boundary of the contact zone; and 2) the review of the circulation and flow patterns within the DAF cell.

It should be noted that the introduction of a third phase such as floc particles would have introduced some stability to the model, a feature recognised in practice by others and presented and reported by Amato *et al.* (2001). However within the constraints of these studies this scenario was not sufficiently detailed to permit reporting at this time.

RESULTS

The results of the plots from the CFD modelling showed that there was little difference between the two temperatures considered and therefore Figures 2(a) to 4(b) show only the results of runs at the maximum flow of 20 Ml/d/cell plus 10% recycle and at 20°C.

It can be seen from Figure 2(a) that the incline baffle as designed and installed results in a general flow path that

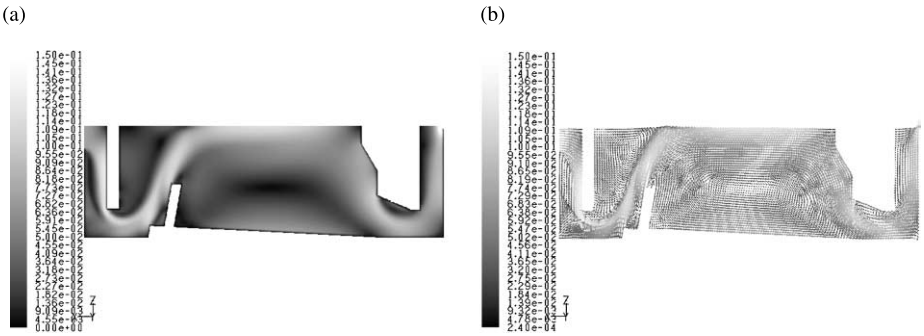

Figure 2 | (a) Velocity contours; (b) velocity vectors.

appears to suggest that the bulk of the tank is bypassed. In contrast Figure 2(b) shows that the classic recirculation is actually present though tending to be throughout the depth of the tank; similar patterns were reported by Lundh *et al.* (2001). If the baffle is extended, as in the case depicted in Figure 3(a), by 500 mm, then not surprisingly, while the general flow path remains the same, the upper region directly beneath the water surface and in practice directly against the underside of any sludge that has floated, shows higher velocity both in terms of the horizontal plane and also over a greater depth. The recirculation flows and corresponding velocity shown in Figure 3(b) when compared with the actually installed baffle arrangement have clearly increased showing both a tighter rotational path and increased tendency to encourage further rotational flows near the upper area of the contact zone and also directly downstream of the upper section of the extended baffle.

These general flow paths and areas of higher turbulence are further highlighted in Figure 4(a) and (b) which show

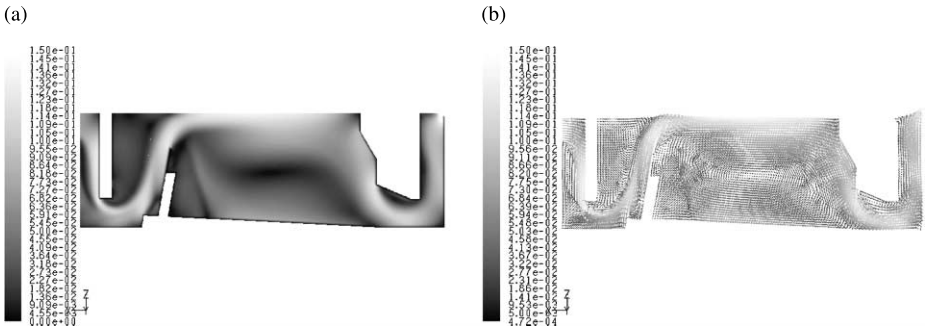

Figure 3 | (a) Velocity contours +500 mm extended baffle; (b) velocity vectors +500 mm extended baffle.

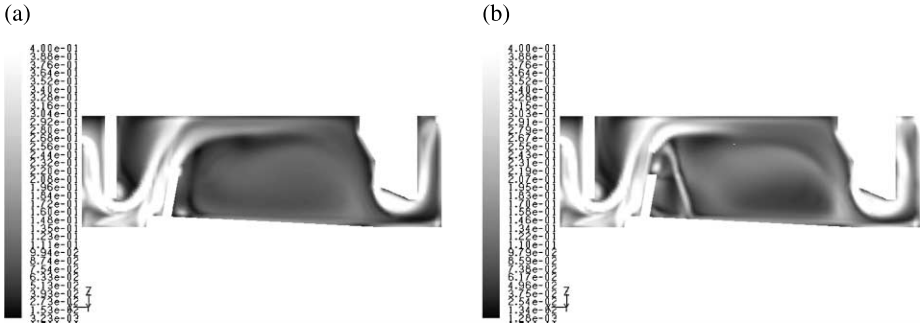

Figure 4 | (a) Vortex contours; (b) vortex contours +500 mm extended baffle.

Table 4 | Incline baffle: Comparison between new design and extended baffle at 20.5 Ml/d and 20°C

	Designed baffle	Extended baffle
T_{10} [s]	152.1	149.0
T_{50} [s]	290.7	300.6
T_{50}/m [ideal = 1]	0.58	0.60
Vorticity magnitude (volume weighted average) [s^{-1}]	0.188	0.204

these effects by the degree and extent of vortex shedding depicted by the intensity of the contours both within the contact zone and immediately downstream particularly in the latter case with the extended baffle arrangement. The impact on the exit region, while not quite so dramatic, is also greater when considering the extended baffle.

In addition to the plots shown in Figures 2–4, the resident time distribution and degree of short circuiting together with the magnitude of vorticity can be derived, a summary of which is presented in Table 4. The data is reported in terms of the standard parameters of T_{10}, T_{50} and T_{50}/m defined as the time taken for 10% or 50% of the flow to exit the tank and the time taken for 50% of the inlet flow to exit the tank divided by the theoretical mean residence time for the tank respectively, and where in an ideal plug flow system T_{50}/m would equal 1.0. In contrast vorticity here has been weighted in accordance with the volume of the tank.

It is clear from the data in Table 4 that the differences are small and appear insignificant; however when the extended baffle was tried in practice this was seen not to be the case and is readily highlighted by the results presented graphically in Figure 5. It can be seen that, as the flow is increased, noting that the recycle rate remained fixed throughout and would have been equivalent to ~10% at maximum flow, both the net load and the velocities over the incline baffle increased and that the apparent small differences suggested in the CFD plots are in fact significant in terms of the subnatant turbidity. The differences are such that, as the flow increased, by the isolation of stream 3 and though the final rate reached per stream was slightly below the maximum design value, the turbidity increased rapidly until the guaranteed maximum limit of 2.0 NTU was exceeded. However in the case of stream 2, which had not been modified from that proposed at the design stage and actually installed, turbidity remained well below 1.5 NTU (95%ile value guaranteed).

It should be noted that the water temperature at the time these tests were carried out was ~10°C and that the subnatant turbidity values derived from the online turbidity meters were corrected to take account of the air present in the sample. It is a common feature of DAF plants that the subnatant will contain air. As this air is released, forming small bubbles, it will register as turbidity even where online meters are fitted with bubble traps. Therefore, while a good indication of the turbidity was derived from the online measurement, these were validated from a small number of spot samples taken from the meters and checked in the laboratory after encouraging any air to escape by gentle agitation prior to measurement, before and during the plant trial; the values are shown in Table 5.

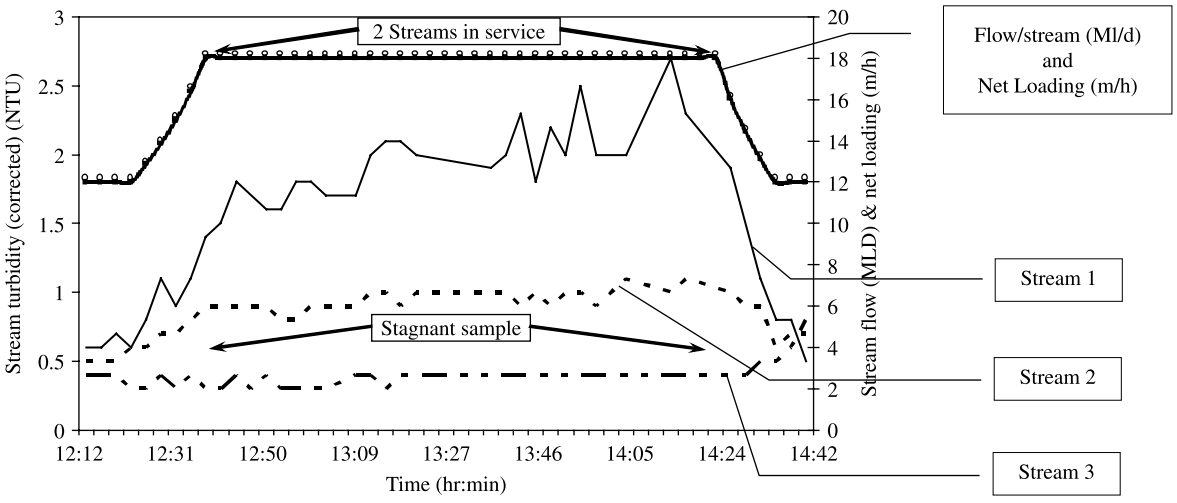

Figure 5 | Designed incline baffle vs. extended baffle (in stream 1).

Table 5 | Designed incline baffle vs. extended baffle (in stream 1): laboratory results

Total plant flow (Ml/d)		36	36	36	36	36
Sample time		10:45	11:10	13:45	14:00	14:20
Streams in service		3	3	2	2	2
Net flow/stream (design 20 Ml/d)		12	12	18	18	18
Stream 1 with extended baffle	Lab (NTU)	0.61	0.64	1.8	1.84	2.1
Stream 2 as designed	Lab (NTU)	0.53	0.56	0.96	0.92	0.97
Stream 3 as designed	Lab (NTU)	0.50	0.56	Off	Off	Off

The original intent of these studies was to establish whether changes to the incline baffle would provide any greater degree of security in achieving the desired subnatant quality. While this was demonstrated not to be the case, initially by the suggestions of an increased risk from the CFD modelling outputs and then more clearly from the actual site trials, the CFD results had raised some additional questions with regard to the design of this and possibly other DAF plants. It was therefore considered appropriate to look further at the modified tank design as installed and to extend the CFD studies to look at other possibilities which could not actually be tried on site because of the practical limitations presented by the existing structures. While a number of areas were considered, such as inlet and outlet baffling arrangements, it was decided to focus on what would be the impact of changing the tank depth.

Figures 6 to 11 show the results of various models at four different water depths: the existing depth of 2.391 m and three others selected arbitrarily at 2.9 m, 3.5 m and 4 m. In all cases the following remained fixed: the gaps created by the various baffles, the flow at 20 Ml/d/stream, the recycle at 10% and the temperature of 20°C. It should be noted that lower temperatures, while not specifically reported here, showed little difference and would not have affected any final conclusions drawn.

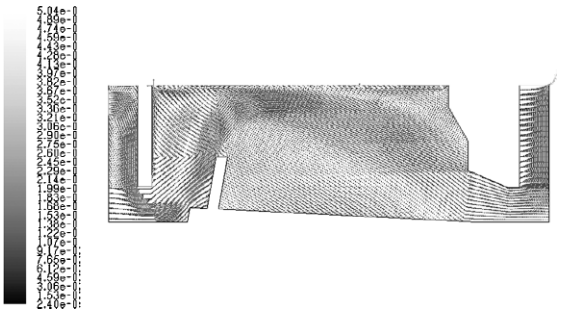

Figure 6 | Velocity vectors at 2.391 m depth.

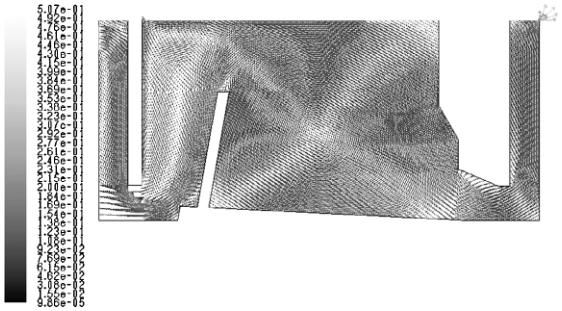

Figure 8 | Velocity vectors at 3.5 m depth.

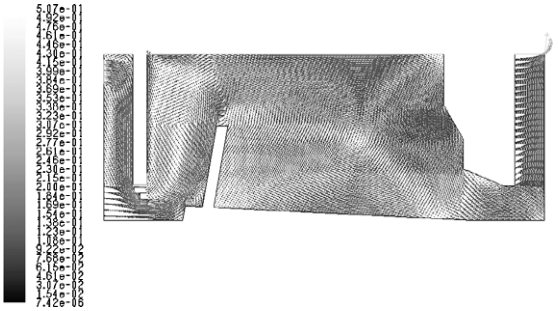

Figure 7 | Velocity vectors at 2.9 m depth.

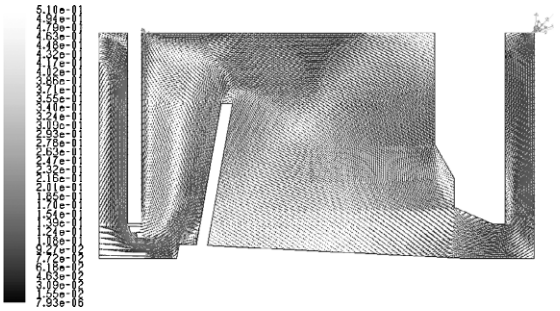

Figure 9 | Velocity vectors at 4.0 m depth.

Figure 10 | Air volume at 3.5 m depth.

It can be seen from Figures 6 to 9 that, as the depth increases, while there is a tendency for the flow to follow the upstream edge of the incline baffle, there is an increase in the degree of rotation that occurs downstream. The plume emerging from the contact zone seen in Figure 6 at the design depth becomes less distinct as the water depth increases; so much so that in Figure 9 there appears to be clear signs of the separation between the white water and the underlying subnatant which, while containing air, will be at a significantly lower concentration.

This is best depicted by the volume fractions in terms of oxygen concentrations shown in Figures 10 and 11, where there is now a clear separation. The separation appears to be at a higher level in Figure 10 but, unlike that which would be seen in the equivalent of Figure 6 where the volume follows the exit plume very closely, here there is no such pattern. These figures all represent a dynamic situation and therefore what is shown is a 'snap shot' of the continually changing environment.

It is obvious that as the water depth is increased one would expect the residence time to increase, but what Table 6 shows is that while the volume increased from 19.8

Figure 11 | Air volume at 4.0 m depth.

Table 6 | Relative impact of changes to HRT and volume with water depth at 10°C

Water depth [m]	2.391	2.9	3.5	4.0
T values: T_{10} [s]	137	160	194	228
T_{50} [s]	265	312	364	414
T_{50}/m	0.61	0.60	0.59	0.59
Increase in T_{10} [%]	–	16.8	41.6	66.4
Increase in volume [%]	–	19.8	43.2	62.7
Vorticity magnitude (volume weighted average) [s^{-1}]	0.185	0.167	0.147	0.136

to 62.7% the equivalent change in the T_{10} time was different and in the range 16.8–66.4%.

If this is taken further, the magnitude of vortices created in each model, per unit volume, may be considered. Assuming that the amount of vortex shedding which occurs (i.e. the source of turbulence and instability in most fluid models) can be related to the likely amount of turbidity measured, then as can be seen from these results, as the volume is increased the vorticity magnitude (normalised by the volume) reduces. When referring to the results presented in Table 4 it can be seen that extending the incline baffle by 500 mm actually increased the vorticity magnitude from 0.188 to 0.204 at a flow of 20.5 Ml/d/stream, suggesting that this was a contributing factor to the difference in turbidity values recorded and presented graphically in Figure 5. While there is no concrete evidence presented here that turbidity and vorticity magnitude are correlated, our experience from these studies and other models would suggest that they are.

CONCLUSIONS

In general as a result of these studies it can be concluded that CFD is a useful tool but that care has to be taken in interpreting the results, since what may appear to be only a small numerical difference between one set of conditions modelled and another, can translate into major deficiencies in practice. Furthermore while DAF plants operating at conventional rates using shallow tanks (i.e. 10 m h^{-1} and $\leq$2.5 m, respectively) may readily achieve the desired product quality, as rates increase, corresponding to

increases in both internal flow velocities and vortex shedding, greater consideration needs to be given to the water depth provided, either by the existing plant or specified by the design engineer. This conclusion has also been inferred by others such as Ta *et al.* (2001) and more recently by Guimet *et al.* (2007).

REFERENCES

Amato, T., Edzwald, J. K., Tobiason, J. E., Dahlquist, J. & Hedberg, T. 2001 An integrated approach to dissolved air flotation. *Water Sci. Technol.* **43**(8), 19–26.

Edzwald, J. K., Tobiason, J. E., Amato, T. & Maggi, L. J. 1999 Integrating high-rate DAF technology into plant design. *J. Am. Water Works Assoc.* **91**(12), 41.

Guimet, V., Broutin, P., Vion, P. & Glucina, K. 2007 *Proc Flotation 2007, 5th International Conference on Flotation in Water and Wastewater Systems*, Seoul, September 2007, pp. 113–119.

Lundh, M., Jönsson, L. & Dahlquist, J. 2001 The flow structure in the separation zone of a DAF pilot plant and the relation with bubble concentration. *Water Sci. Technol.* **43**(8), 185–194.

Marshall, E. M. & Bakker, A. 2002 *Computational Fluid Mixing*. Fluent Inc., Lebanon, New Hampshire.

Ta, C. T., Beckley, J. & Eades, A. 2001 A multiphase CFD model of DAF process. *Water Sci. Technol.* **43**(8), 153–157.

Yakhot, V. & Orszag, S. A. 1986 Renormalisation group analysis of turbulence: 1 basic theory. *J. Sci. Comput.* **1**(1), 1–51.

First received 21 January 2008; accepted in revised form 10 April 2008. Available online December 2008